



Global Biogeochemical Cycles

RESEARCH ARTICLE

10.1002/2017GB005668

This article is a companion to Izett and Fennel (2018), <https://doi.org/10.1002/2017GB005667>.

Key Points:

- Export of fresh water and nutrients from rivers to the open ocean is estimated on local and global scales
- Export is most efficient within 15 degrees of the equator and where shelves are narrow
- Globally, less than 60% of all riverine fresh water and nutrients are exported directly to the open ocean

Supporting Information:

- Supporting Information S1
- Data Set S1

Correspondence to:

J. G. Izett,
j.g.izett@tudelft.nl

Citation:

Izett, J. G., & Fennel, K. (2018). Estimating the cross-shelf export of riverine materials: Part 2. Estimates of global freshwater and nutrient export. *Global Biogeochemical Cycles*, 32, 176–186. <https://doi.org/10.1002/2017GB005668>

Received 11 MAR 2017

Accepted 27 AUG 2017

Accepted article online 19 DEC 2017

Published online 5 FEB 2018

Estimating the Cross-Shelf Export of Riverine Materials: Part 2. Estimates of Global Freshwater and Nutrient Export

Jonathan G. Izett^{1,2}  and Katja Fennel¹ 

¹Department of Oceanography, Dalhousie University, Halifax, Nova Scotia, Canada, ²Department of Geoscience and Remote Sensing, Delft University of Technology, Delft, The Netherlands

Abstract Rivers deliver large amounts of fresh water, nutrients, and other terrestrially derived materials to the coastal ocean. Where inputs accumulate on the shelf, harmful effects such as hypoxia and eutrophication can result. In contrast, where export to the open ocean is efficient riverine inputs contribute to global biogeochemical budgets. Assessing the fate of riverine inputs is difficult on a global scale. Global ocean models are generally too coarse to resolve the relatively small scale features of river plumes. High-resolution regional models have been developed for individual river plume systems, but it is impractical to apply this approach globally to all rivers. Recently, generalized parameterizations have been proposed to estimate the export of riverine fresh water to the open ocean (Izett & Fennel, 2018, <https://doi.org/10.1002/2017GB005667>; Sharples et al., 2017, <https://doi.org/10.1002/2016GB005483>). Here the relationships of Izett and Fennel (2018), <https://doi.org/10.1002/2017GB005667> are used to derive global estimates of open-ocean export of fresh water and dissolved inorganic silicate, dissolved organic carbon, and dissolved organic and inorganic phosphorus and nitrogen. We estimate that only 15–53% of riverine fresh water reaches the open ocean directly in river plumes; nutrient export is even less efficient because of processing on continental shelves. Due to geographic differences in riverine nutrient delivery, dissolved silicate is the most efficiently exported to the open ocean (7–56.7%), while dissolved inorganic nitrogen is the least efficiently exported (2.8–44.3%). These results are consistent with previous estimates and provide a simple way to parameterize export to the open ocean in global models.

1. Introduction

Freshwater plumes associated with river mouths are ubiquitous along the world's coastlines. Along with large volumes of fresh water, they deliver large amounts of nutrients, sediments, and pollutants from land to the coastal ocean (from weathering and erosion as well as agricultural and industrial runoff). Whether this material accumulates and is processed on continental shelves (defined here as water shallower than 200 m) or delivered to the open ocean is important for understanding local and global freshwater and nutrient budgets. In cases of high nutrient delivery but low efficiency of cross-shelf export, riverine nutrients accumulate leading to eutrophication, and potentially detrimental effects such as harmful algal blooms and hypoxia (e.g., Diaz and Rosenberg, 2008; Doney, 2010; Galloway et al., 2004; Seitzinger et al., 2010). In the case of efficient cross-shelf export, the risk of these effects is reduced (e.g., Chen et al., 2003; Gruber & Galloway, 2008).

The need for understanding the fate of river-borne materials is becoming ever more important. Globally, nutrient loads to the coastal ocean have increased dramatically compared to preindustrial levels due to growing use of industrial fertilizers to feed the expanding world population and other human activities (Diaz and Rosenberg 2008; Galloway et al., 2004; Seitzinger et al., 2010). Nitrogen delivery by rivers, for example, increased by 40% from 1970 to 2000: a trend that is predicted to continue (Galloway et al., 2004). How and where these materials are transported will determine their impact on coastal systems and global budgets.

The difficulty in obtaining a global representation of river plume export is illustrated by its treatment in the current global models. At present, global model resolution is too coarse to capture the relatively small-scale features of the coastal ocean—including river plumes—meaning they are unable to directly simulate the transport of riverine nutrients and the coupled transport processes across the shelf break. Cotrim da Cunha et al. (2007) illustrate how important accurate nutrient input is for global models. While their coastal resolution is still coarse, they compare the impact of different nutrient input scenarios ranging from the extreme case of zero nutrient input to a high input scenario representative of a global human population

of 12 billion people. Relative to current nutrient input levels, the high input scenario leads to an increase in open ocean productivity of roughly 5%, and a 10% increase over the zero-input scenario. Bernard et al. (2011) include heterogeneous riverine-dissolved silica inputs and highlight the dependence on regional delivery patterns and the subsequent formation of ocean “hot spots” of oceanic silica.

Still, in many cases, including in climate models, freshwater and nutrient export from the coastal to the open ocean must be parameterized or ignored, with many models assuming an “all or nothing” approach (Izett & Fennel, 2018). Simple box models (e.g., Garvine & Whitney, 2006) can be useful on a local scale, but they are impractical to employ globally. Conversely, global mass balance models (e.g., Laruelle et al., 2009; Rabouille et al., 2001) can be used to assess generalized coastal nutrient budgets and fluxes but do not allow for consideration of individual river properties and require many simplifying assumptions about the physical and biogeochemical processes taking place on a global scale.

Recently, Sharples et al. (2017) proposed a simple parameterization to describe riverine export to the open ocean using the S_p number: the ratio of a plume’s width to the local shelf width. Where the S_p number is larger than 1 (i.e., where the plume is wider than the shelf), Sharples et al. (2017) predict that export of riverine material is efficient and direct. Using empirical formulae to calculate shelf processing times and biogeochemical nutrient removal, Sharples et al. (2017) conclude that efficient transport occurs primarily within 20° of the equator, and along continental margins where shelves are narrow. They estimate that approximately 75% dissolved inorganic nitrogen (DIN) and 80% dissolved inorganic phosphorus (DIP) delivered by rivers globally reach the open ocean. Their new estimates have already been implemented in a global reassessment of nitrogen inputs to the open ocean by Jickells et al. (2017) after a previous analysis assumed no open-ocean delivery of nitrogen from rivers. While the simplified approach allows for extremely easy and straightforward estimation of the export and retention of riverine material, however, their arguments were not tested with a numerical model and only rely on scaling assumptions.

We extended the simple framework proposed by Sharples et al. (2017) in the first part of this paper (Izett & Fennel, 2018) through a series of idealized river plume simulations in which latitude, discharge, wind speed/direction, and tidal forcing were varied. The results indicated that latitude is the strongest influence in determining cross-shelf and alongshore export of fresh water (due to the control of the Coriolis force) such that high-latitude rivers have extremely limited export efficiency, regardless of the other forcing (less than 50% of fresh water above 30°, and as less than 5% above 45° for shelves wider than 65 km). From the simulation results, we developed empirical relationships to parameterize plume export as a function of S_p , with low S_p rivers (those with wide shelves or high latitudes) showing limited cross-shelf export of riverine material. Our objective in this second manuscript is to apply these relationships to global rivers in order to demonstrate their use and to estimate the export of riverine fresh water and nutrients to the open ocean in a global, general sense. In our assessment, we focus on the direct export of materials within river plumes, as opposed to subsequent transport processes that occur on longer timescales after riverine nutrients have undergone biogeochemical transformation on the shelf.

2. Methods

2.1. Estimating Nutrient Export and Retention

In Part 1 (Izett & Fennel, 2018), we presented four primary relationships that, in conjunction, can be used to estimate the cross-shore and alongshore export of fresh water as a fraction of a river’s discharge (E_X^{FW} and E_A^{FW} , respectively), the export timescale (T_E ; i.e., how long it takes for cross-shelf export to occur), and the Rossby radius of a plume (R_o). Only simple and easily measured parameters need to be known a priori, such as river discharge. The relationships were obtained by applying statistical regressions to the output from numerical simulations of idealized river plumes.

To estimate the freshwater export efficiency, we use equations (7) and (8) from Izett and Fennel (2018), with the cross-shelf export depending on S_p ($4.3R_o/W_S$, where W_S is the local shelf width; Sharples et al., 2017) such that export is higher for rivers that are large in relation to the shelf ($S_p > 1$; low latitude or narrow shelves):

$$E^{\text{FW}} = \frac{\zeta - 1}{\zeta}$$

$$\text{where } \zeta = aS_p^{1/2} + b. \quad (1)$$

The regression coefficients a and b are, respectively, 1.1 ± 0.4 and 0.5 ± 0.3 . Similarly, the alongshore export efficiency is a function of the Rossby radius (R_o), which provides an indication of the amount of deflection by the Coriolis force (the smaller the Rossby radius, the greater the deflection, resulting in increased alongshore transport), with $a = 1.6 \pm 0.2 \text{ km}^{1/2}$ and $b = -0.10 \pm 0.02$:

$$E_A^{\text{FW}} = \begin{cases} aR_o^{-1/2} + b & R_o^{-1/2} \geq -b/a \\ 0 & R_o^{-1/2} < -b/a \end{cases} \quad (2)$$

We restrict our estimates such that $E_A^{\text{FW}} \leq 1 - E_X^{\text{FW}}$ and calculate the Rossby radius as

$$R_o = \sqrt{\frac{g}{f^2 \rho_o} \Delta \rho h}, \quad (3)$$

which depends on latitude through the Coriolis parameter (f), the ambient density (ρ_o —assumed to be $1,025 \text{ kg m}^{-3}$), and gravitational acceleration (g). $\Delta \rho h$ (the product of the difference in density between the plume and ambient water, and the depth of the plume) is estimated from discharge (Q) and the Coriolis parameter (f) (equation (10) in Izett & Fennel, 2018), where $a = 70 \pm 6 \text{ kg s m}^{-7/2}$ and $b = 43 \pm 5 \text{ kg m}^{-2}$:

$$\Delta \rho h = a\sqrt{Qf} + b. \quad (4)$$

Finally, the export timescale in equation (3) is estimated with equation (9) from Izett and Fennel (2018), with $a = 0.2 \pm 0.1$ days and $b = 0.8 \pm 1.3$ days:

$$T_E = aS_p^{-3} + b, \quad (5)$$

such that the larger the river in relation to the shelf (increasing S_p), the more rapidly material is exported. In conjunction with equation (1), this means that rivers with high volume export of fresh water also export the most quickly such that nutrient retention on the shelf is low.

The above relationships allow for the simple estimation of freshwater export. In order to estimate nutrient export, however, the removal of nutrients on the shelf must also be estimated. To do so, we describe the plume as a constant and well-mixed volume, V (m^3), which is assumed to be in steady state with respect to nutrient and water fluxes. Given the rate of inflow, Q ($\text{m}^3 \text{ s}^{-1}$), the nutrient concentration in the inflow, N^{in} (mmol m^{-3}), and a constant nutrient removal rate within the plume, r (s^{-1}), the nutrient budget of the plume is

$$\frac{\partial NV}{\partial t} = QN^{\text{in}} - rNV - QN = 0 \quad (6)$$

where N is the outgoing nutrient concentration and is equal to $(1 - F_r)N^{\text{in}}$. The export timescale is $T_E = V/Q$. The total fraction of nutrients removed, F_r , is then

$$F_r = \frac{rT_E}{1 + rT_E}. \quad (7)$$

The inverse of the removal rate, r , is the processing timescale, which is an indicator of the time it takes for nutrients to be removed from the system through biogeochemical processing and transformations. $1 - F_r$ is the resulting fraction of nutrients that remains in the plume.

The total amount of nutrient export (Γ_D^{Nut}) in a given direction, D (either cross-shelf, X , or along shelf, A), is the product of the incoming nutrient load from the river (N^{in}) and the efficiency of nutrient export (E_D^{Nut}). E_D^{Nut} depends not only on the freshwater export efficiency (E_D^{FW}) but also on the additional scaling factor $(1 - F_r)$ that depends on the rate of removal (r), and the export timescale (T_E)

$$\begin{aligned} \Gamma_D^{\text{Nut}} &= E_D^{\text{Nut}} N^{\text{in}} \\ &= \frac{1}{1 + rT_E} E_D^{\text{FW}} N^{\text{in}} \end{aligned} \quad (8)$$

This relationship accounts for the fact that nutrient export is controlled by both removal processes and by physical plume circulation.

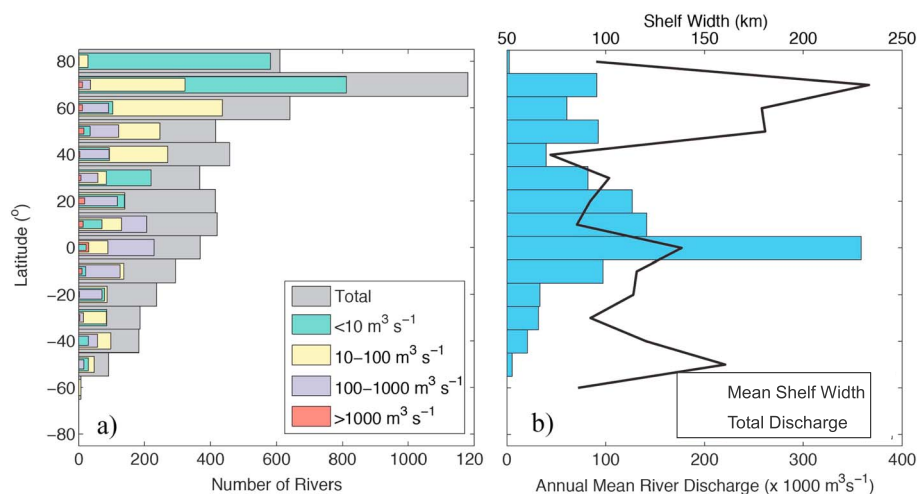


Figure 1. Global river properties. (a) Histogram of the number of GlobalNEWS rivers in 10° latitude bands grouped by discharge. (b) ETOPO1 mean shelf width (black line) and total GlobalNEWS freshwater discharge (blue bars) for 10° latitude bands.

We estimate nutrient export for a range of processing rates from the lower limit of no nutrient processing (i.e., for a conservative tracer; $r = 0 \text{ d}^{-1}$) to an upper limit in processing rate of 0.75 d^{-1} , which is 5 times faster than the rate used by Rabouille et al. (2001) in their estimates of globally averaged nutrient uptake by phytoplankton.

Our estimates are deliberately kept general to avoid making many assumptions about the different biogeochemical processes that take place on continental shelves. Processes such as sedimentation/burial and denitrification constitute the primary sinks of nutrient inputs (e.g., Fennel et al., 2006), but we do not explicitly consider their role, which has a significant regional variability. Instead, our simple, general approach of assuming a range of different processing rates provides an envelope on which to base nutrient export estimates.

2.2. Global River Data

As in Sharples et al. (2017), we estimate global freshwater and nutrient export using discharge and nutrient load information from the GlobalNEWS database (Mayorga et al., 2010). GlobalNEWS contains approximately 5,800 rivers that discharge directly into the ocean. Available information includes river locations, discharges, and nutrient loads. From this, we estimate the export of fresh water as well as global nutrient export for dissolved inorganic and organic nitrogen (DIN and DON), dissolved inorganic and organic phosphorus (DIP and DOP), dissolved organic carbon (DOC), and dissolved silicate (DSi).

In addition to the river data from GlobalNEWS, we used NOAA's ETOPO1 topography (Amante & Eakins, 2009) to estimate the shelf width for each river as the distance from the river mouth to the 200 m isobath. Shelf widths ranged from just tens of kilometers (e.g., 20 km for the Congo River) up to hundreds of kilometers (e.g., for Arctic Rivers).

3. Results

3.1. Estimating Local Freshwater and Nutrient Budgets

Using the idealized relationships outlined in Izett and Fennel (2018) and summarized in section 2.1, we estimated the export efficiency of all rivers in the GlobalNEWS database (Mayorga et al., 2010). Globally, rivers vary significantly in discharge, nutrient load, and latitude and, hence, are expected to vary in plume dynamics and cross-shelf export efficiency (Figure 1). Riverine nutrient loads and freshwater discharge covary (larger rivers deliver more nutrients to the coastal ocean); however, nutrient concentrations are independent of river discharge, with often greater nutrient concentrations in the low latitude to midlatitude of the Northern Hemisphere. Most of the world's rivers are small (less than $100 \text{ m}^3 \text{ s}^{-1}$ discharge), with overall more rivers

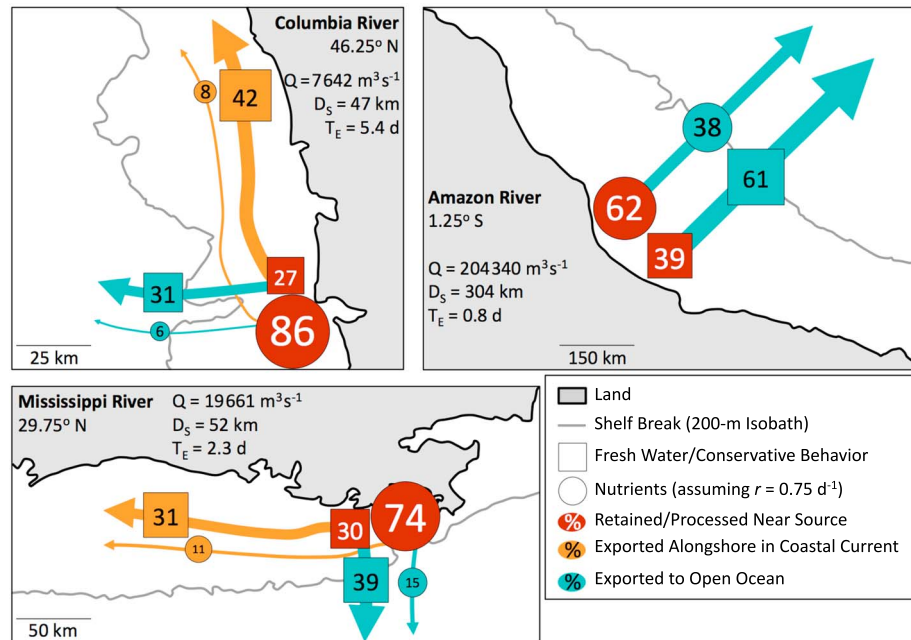


Figure 2. Estimated freshwater and nutrient budgets for the Amazon River, Mississippi River, and Columbia River plumes. The shelf width was calculated from river mouth to the 200 m isobath. Nutrient processing is assumed to occur at a removal rate of 0.75 d^{-1} .

in the Northern Hemisphere. Total freshwater discharge is also higher in the Northern Hemisphere, as are shelf widths. The Amazon River dominates global discharge, delivering approximately one sixth of the global annual freshwater input.

Figure 2 presents the individual freshwater and nutrient budgets for the Amazon, the Mississippi, and the Columbia Rivers. These three rivers are among the largest 20 rivers in the GlobalNEWS database by annual discharge (first, Amazon; sixth, Mississippi; and twentieth, Columbia) and span a range of latitudes and shelf widths with 1.25°S and 304 km, 29.75°N and 52 km, and 46.25°N and 47 km, respectively. The Amazon flows onto a wide shelf but is still the most efficient cross-shelf exporter, with up to 31–73% cross-shelf export efficiency for fresh water (12–73% nutrients) and negligible downstream transport in the coastal current; this is due to its high discharge and close proximity to the equator leading to minimal deflection by the Coriolis force. We estimate much greater downstream advection for the Mississippi and Columbia Rivers, and much higher overall shelf retention. The Columbia River has the greatest downstream transport, with 34–51% of the river discharge advected away from the source region in the coastal current due to the strong influence of the Coriolis force (it is the highest latitude of the three rivers). The role of the export timescale is apparent, with nutrients being significantly depleted for the Mississippi and Columbia Rivers, which have export timescales of 2.5 and 5.7 days, respectively, as opposed to the Amazon River, whose export timescale is less than 1 day.

3.2. Estimates for Socioeconomic Regions

As an example of regional estimates, we present combined freshwater budgets for all rivers in four socioeconomic regions of the Northern Hemisphere: eastern and western North America, northwestern Europe, and south Asia (Figure 3). Of the four regions, western North America has the narrowest shelf widths (in some cases, less than 10 km) due to the presence of active subduction zones. As a result, S_p is high, resulting in the greatest cross-shelf export of all regions considered (33%) and lower processing timescales (days to weeks). The high latitudes of the rivers mean that the remainder of the riverine material that is retained on the shelf is transported alongshore in the coastal current (49% of all input material), rather than being retained near the source (just 18%).

South Asia—which has high nutrient inputs due to agriculture and land use practices—is the lowest-latitude region whose rivers are therefore less influenced by deflection from the Coriolis force. However, wider shelves (such as the Yangtze that flows into the East China Sea) than the West Coast of North

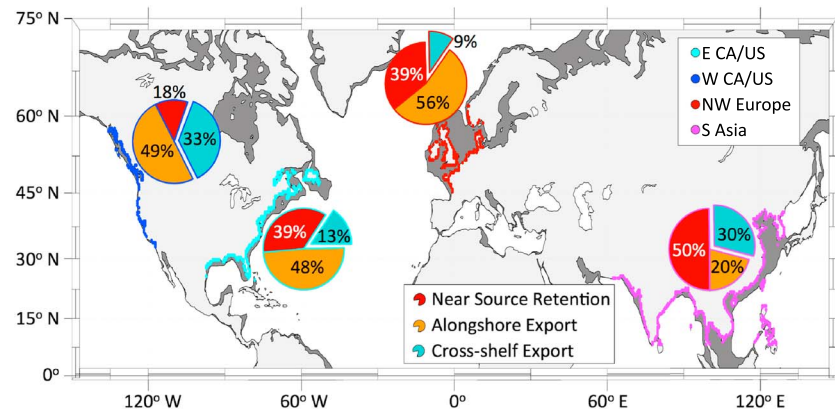


Figure 3. River mouth locations and freshwater budgets for four socioeconomic regions: East and West Coasts of North America, northwestern Europe, and south Asia. Continental shelves are shown in dark gray.

America mean that the region has comparable S_p and the cross-shelf export is similar (30%). The low-latitude (weaker Coriolis force and large R_o) and wide shelves also mean that the remaining material is retained near the source in the highest proportion of the four regions (60%), rather than being advected alongshore in the coastal current.

The highly industrial and developed regions of eastern North America and northwestern Europe are at higher latitudes and have very wide shelves (particularly, the North Sea region of northwestern Europe where rivers such as the Rhine flow). As a result, S_p in these regions is small, with eastern North America and northwestern Europe having just 13% and 9% cross-shelf export, respectively, and export timescales on the order of years. A significant fraction is transported downstream in the coastal current due to higher latitudes, but roughly 40% of the riverine material is retained and processed near the source.

Two smaller regions within the eastern North American zone are the Gulf of Mexico and the Mid-Atlantic Bight. Both regions have high riverine nutrient inputs from the continental United States (including the Mississippi River from section 3.1 that flows into the Gulf of Mexico) and regularly experience hypoxic conditions. Due to wide shelves, S_p is small for the majority of rivers in these regions, and cross-shelf export is as such greatly restricted. We estimate up to 64% cross-shelf nutrient export for the Gulf of Mexico assuming no processing, but as low as 4% export when nutrient processing is high. The Mid-Atlantic Bight, which is at higher latitudes than the Gulf of Mexico, has much lower nutrient export, with just 0–28% of the material being exported to the open ocean.

3.3. Global Estimates of Freshwater and Nutrient Export

Calculating the freshwater and nutrient export for each river in the GlobalNEWS model, we obtained estimates for the global freshwater and nutrient export in river plumes. We estimate that between 15 and 53% of the riverine fresh water is exported to the open ocean (equivalent to approximately $6\text{--}20 \times 10^3 \text{ km}^3$ annually). Figure 4 shows that the highest efficiencies are confined to a narrow band spanning roughly 15° on either side of the equator and on the narrow active margins of the continental shelves (such as the West Coast of North America). In general, the estimated cross-shelf export of fresh water is higher in the Northern Hemisphere than the Southern Hemisphere, with a decrease in cross-shelf export and corresponding increase in alongshore export with increasing distance from the equator in both hemispheres. Cross-shelf export is dominant in the low latitudes. Retention near the source peaks in the midlatitudes in both hemispheres. Alongshore export is greatest in the higher latitudes. Within 10° of the equator, 60% riverine fresh water is exported to the open ocean, while 60% of fresh water is retained in the coastal current above 45° .

Even assuming conservative export, the upper bounds of global nutrient export are low. DSI is exported globally with the highest efficiency of all the nutrients (18.2–56.4%), while DIN has the lowest conservative export efficiency (7.3–44.3%). With an assumed processing rate of 0.75 d^{-1} , the estimates drop to 7.0–44.3% and 2.8–24.9%, respectively, suggesting high shelf retention of nutrients. Export efficiencies differ among

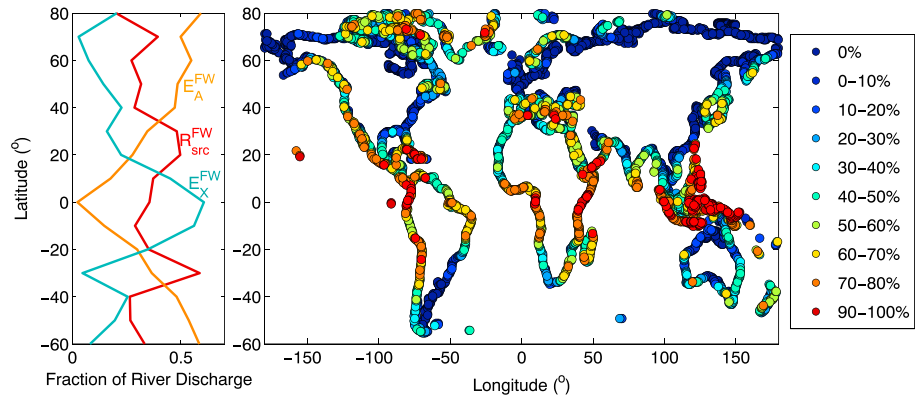


Figure 4. Estimated global freshwater export. (a) Cross-shelf and alongshore export (E_X and E_A) and near source retention (R_{src}) of riverine fresh water in 10° latitude bands. (b) Cross-shelf freshwater export efficiency beyond the 200 m isobaths for individual rivers in the GlobalNews model.

nutrients due to variations in nutrient delivery. For example, DSi delivery is related to river discharge such that global distribution of DSi delivery is also very similar to the overall freshwater distribution. DSi is primarily delivered to the ocean near the equator where export is efficient, with the Amazon River being the largest proportion of DSi (Figure 5b). DIN, on the other hand, is delivered to the ocean primarily above 20°N (Figure 5a), which is related to the regions of high agricultural activity in the Northern Hemisphere but outside of the region of efficient export.

Global comparisons are presented in Figure 5 for DIN and DSi under different removal scenarios: no removal (conservative export), low removal ($r = 0.15 \text{ d}^{-1}$; used by Rabouille et al., 2001 as a global rate of shelf uptake of DIN by phytoplankton), and high removal ($r = 0.75 \text{ d}^{-1}$; at this rate global nutrient export begins to level off and is less sensitive to further increases in r). The highest export occurs in the low latitudes and decreases with higher latitudes. Under the removal scenarios, the combination of long export timescales and already reduced freshwater export efficiency at high latitudes results in very little to no estimated nutrient export above 30°.

For the highest and lowest processing rates ($r > 10 \text{ d}^{-1}$ and $r < 0.01 \text{ d}^{-1}$, corresponding to processing timescales of less than 0.1 day or greater than 100 days), the global riverine export is not very sensitive to small changes in r . Between processing timescales of 1 day to a few months, however, export is sensitive to the rate

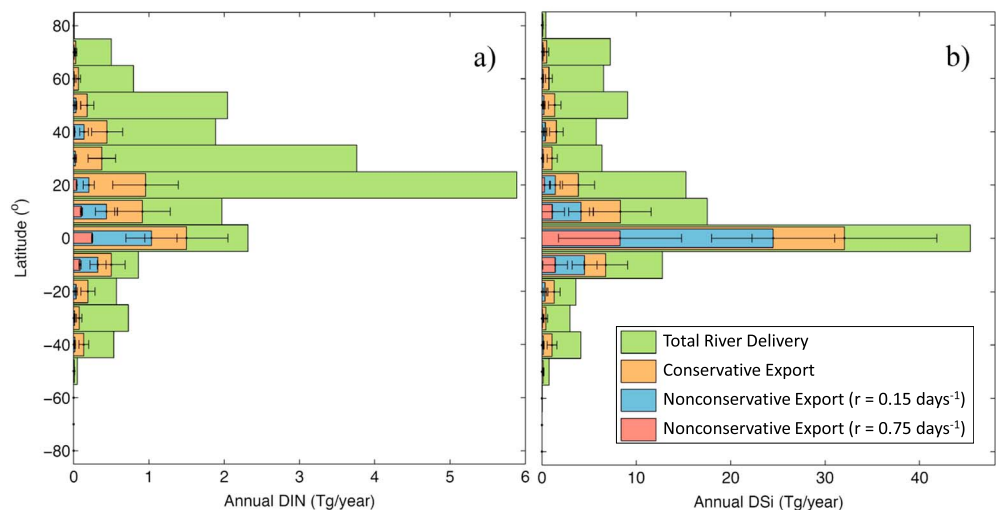


Figure 5. Comparison of total (a) DIN and (b) DSi delivery and cross-shelf export in 10° latitude bands, calculated for individual rivers following equation (8).

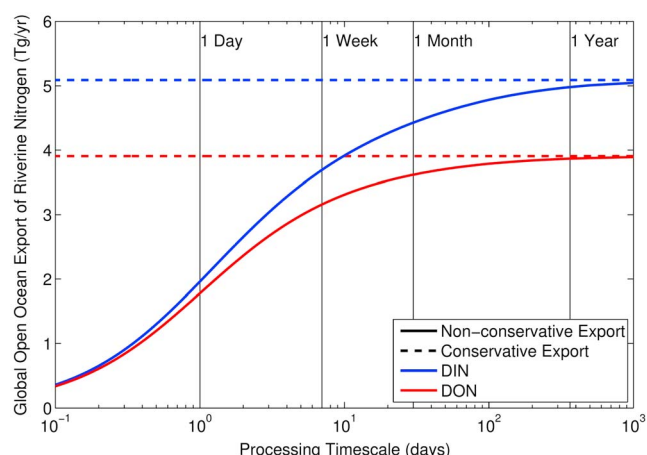


Figure 6. Global export of DIN and DON for different shelf processing timescales. The dashed line represents the conservative export.

chosen, with a significant decrease in exported nutrients for shorter processing timescales (Figure 6). Within this range, increasing the removal rate by 1 order of magnitude results in approximately a factor of 2 decrease in the number of rivers that are estimated to export to the open ocean and an equivalent decrease in the overall nutrient export. Of the six nutrients considered, DIN and DIP are depleted most rapidly for the lowest nutrient removal rates, while DSi and DOC not only have the largest riverine loads but also are exported with the greatest efficiency. It should be stressed that the difference in exported loads is due to geographical variation in nutrient delivery (e.g., an efficient river may have high DSi load but low DIN) rather than differences in nutrient processing rates that we assume are the same for all nutrients.

The overall ranges of nutrient export estimates (from the lowest at $r = 0.75 \text{ d}^{-1}$ to the highest under conservative behavior) are presented in Table 1, for select individual rivers/regions, and in 10° latitude bands. The supporting information further contains all of the calculated estimates in Data Set S1 for each river in the GlobalNEWS model.

4. Discussion

Our methodology allows for the estimation of freshwater and nutrient export on a range of scales: from individual rivers to regional scales and globally. Where available, our estimates are largely in agreement with previously published estimates.

We present export estimates of fresh water and nutrients for three individual rivers—the Amazon, Columbia, and Mississippi—in Figure 2. DeMaster and Aller (2001) report 50%, 100%, and 92% of the total nitrogen, phosphorus, and silica delivered to the Amazon shelf, respectively, and exported across the shelf to the open ocean (as determined through a series of transects). Our estimate of 12–73% riverine nutrient export (Table 1) spans very rapid processing ($r = 0.75 \text{ d}^{-1}$) to conservative export ($r = 0 \text{ d}^{-1}$). These estimates are consistent with DeMaster and Aller (2001) assuming that phosphorous and silicate behave almost conservatively on the Amazon shelf, while nitrogen is subject to moderate rates of processing.

Table 1
Export Estimates of Fresh Water and Nutrients, for Select Individual Rivers/Regions, and for 10° Latitude Bands Centered as Indicated

	FW	DIN	DON	DIP	DOP	DOC	DSi
Global	15–53%	3–44%	6–52%	4–46%	6–52%	6–52%	7–56%
Amazon	31–73%			12–73%			
Mississippi	19–69%			7–69%			
Gulf of Mexico	14–65%	5–64%	5–64%	4–63%	4–63%	5–64%	5–64%
Mid-Atlantic Bight	0–28%	0–28%	0–28%	0–28%	0–28%	0–28%	0–28%
80°N	5–42%	1.5–35%	1.5–38%	1–39%	1.5–38%	1.5–38%	1–41%
70°N	0.5–17%	0.5–17%	0.2–16%	0.2–12%	0.2–16%	0.2–16%	0.5–20%
60°N	1–23%	0.2–22%	0.4–22%	0.2–23%	0.4–23%	0.3–21%	0.5–28%
50°N	1.5–36%	0.4–29%	0.5–34%	0.4–22%	0.5–35%	0.6–34%	1–37%
40°N	4–45%	2–45%	2–44%	3–46%	2–45%	1.5–44%	2–48%
30°N	0.5–38%	0.2–32%	0.3–36%	0.6–33%	0.2–35%	0.2–37%	0.5–40%
20°N	5–47%	1–43%	2–47%	1.5–44%	2–46%	2–47%	3–49%
10°N	13–62%	7–63%	5–62%	8–65%	5–62%	5–62%	7–63%
0°	32–72%	11–71%	12–72%	12–72%	12–72%	12–72%	14–73%
10°S	34–69%	11–69%	13–70%	7–66%	13–70%	13–68%	11–66%
20°S	4–55%	1.5–55%	1.5–55%	2–54%	1.5–55%	1.5–55%	2–55%
30°S	1–31%	0.5–33%	0.5–32%	1–38%	0.3–31%	0.2–31%	0.5–37%
40°S	3–48%	1–48%	1–47%	1–48%	1–48%	1–47%	1–49%
50°S	0.2–44%	0–45%	0.1–44%	0–48%	0.1–44%	0.1–44%	0–45%
60°S	0–37	0–39%	0–37%	0–37%	0–37%	0–37%	0–37%

Note. The minimum nutrient value is obtained assuming a shelf processing rate of 0.75 d^{-1} , with the upper estimate assuming conservative nutrient behavior on the shelves ($r = 0 \text{ d}^{-1}$). See supporting information for estimates of all rivers (Data Set S1).

Zhang et al. (2012) conducted a detailed numerical study of the Mississippi River and Atchafalaya River outflows onto the shelf in the northern Gulf of Mexico. Using two numerical dyes, they tracked the freshwater discharge from the two rivers and estimated the cross-shelf export beyond the 100 m isobath to be approximately 57% and 36% of the riverine discharges, respectively. Our estimates of cross-shelf export of up to 61% and 42% for the Mississippi and Atchafalaya, respectively, agree very well with the estimates of Zhang et al. (2012).

The limits of the methodology become apparent, however, when comparing our estimates to regional shelf nutrient budgets. For example, Lehrter et al. (2013), Xue et al. (2013), and Fennel et al. (2006) report freshwater and nutrient budgets for the northern and whole Gulf of Mexico shelf, and the Mid-Atlantic Bight, respectively. Each of these studies considers inputs from multiple rivers and nonriverine sources such as onwelling from the open ocean and accounts for the possibility of riverine nutrients being exported by other means than direct export in the river plume, for example, after being mixed into shelf water or being incorporated into organic matter. Our simple approach cannot account for these processes; complete regional nutrient budgets as presented in Lehrter et al. (2013), Xue et al. (2013), and Fennel et al. (2006) are needed for this purpose.

In section 3.2 we present regional estimates for four socioeconomic regions—eastern and western North America, northwestern Europe, and south Asia (Figure 3)—as further examples of how the methodology can be applied on regional scales. To the best of our knowledge, there are no published previous estimates for comparison; however, these first estimates are enlightening. A clear difference is seen between the western coast of North America—which we estimate to have the highest proportion of material directly exported across the comparatively narrow shelf—and the other three regions that are estimated to have very high near-source retention.

We estimate that globally just 15–53% of the riverine fresh water is exported to the open ocean. The upper limits of our nutrient export estimates are similar to that of fresh water, but the lower limits are much less due to shelf processing with ranges of 2.8–44.3% for DIN, 5.6–51.8% for DON, 3.5–45.9% for DIP, 5.5–51.9% for DOP, 5.7–52.3% for DSi, and 7.0–56.4% for DOC.

The highest export efficiency occurs within a narrow band extending approximately 15° north and south of the equator where the low latitude dictates large Rossby radii (Figure 4). High export rates also occur at active margins where the shelf is narrow (high S_p regions). This is consistent with Sharples et al. (2017) who predict most cross-shelf export occurs within 20° of the equator and along narrow shelves. Interestingly, the two largest rivers, the Amazon and the Congo, which account for approximately 20% of the world's freshwater discharge, are very close to the equator where export efficiency is high; however, the majority of global rivers fall outside of the regions of efficient export and have much weaker discharges, such that much of the riverine material is retained on the shelf.

Where a greater fraction of the plume's fresh water reaches the shelf break (higher freshwater export efficiency) the export timescales are also shorter. Hence, rivers that transport more material to the open ocean also do so faster, meaning less nutrient removal can occur before the plume reaches the shelf break. Conversely, rivers that have high shelf retention also have long export timescales, meaning that by the time the river plumes reach the shelf break, they have been subjected to nutrient removal by biogeochemical processing. Only the plumes with rapid export (as seen near the equator or along narrow shelves) can effectively transport nutrients to the deep ocean when processing rates are high.

The global export estimates are most sensitive to the processing rate within the range of 0.01 d^{-1} to 1 d^{-1} . This corresponds to a range of processing timescales from one to 100 days—the same as the range of global export timescales. Within this range, riverine nutrient export changes by a factor of approximately 10. However, the global estimates are not very sensitive to this choice, for example, values of $r = 1 \text{ d}^{-1}$ and $r = 0.1 \text{ d}^{-1}$ (an order of magnitude difference) change global nutrient export by only a factor of 2. For processing timescales above 100 days and below 1 day, the estimated nutrient exports are approximately constant. For rapid processing ($r > 1 \text{ d}^{-1}$), we estimate very little nutrient export. At very low processing rates ($r < 0.01 \text{ d}^{-1}$) nutrient export expectedly approaches the conservative levels.

Most of the global riverine nutrient supply is delivered to the ocean through rivers in the Northern Hemisphere (80% of all riverine DIN, for example, is delivered in the Northern Hemisphere). The estimates

of global nutrient export efficiencies are greatest for dissolved silica (DSi; 7.0% for high processing and up to 56.4% assuming conservative export), because the highest riverine loads occur in the low latitudes where export timescales are short and freshwater export is the most efficient (Figure 5a). Conversely, DIN is predominantly delivered in the midlatitude to high latitude of the Northern Hemisphere: outside the zone of efficient plume export (Figure 5b), making it the least efficiently exported nutrient.

The qualitative global patterns of shelf retention and export timescales correspond to global patterns of hypoxia and eutrophication (e.g., Diaz & Rosenberg, 2008). In particular, along the coast of northwestern Europe, the eastern United States, and southern Asia, where the shelf is wide, the majority of river water is retained on the shelf (87%; Figures 3 and 4), with long export timescales (on the order of several months to years). As a result, river-borne nutrients, which are delivered in high amounts to these areas, accumulate on the shelves, driving eutrophication and hypoxia. A quantitative comparison between our estimates of shelf retention and global patterns of hypoxia and eutrophication is beyond the scope of this current work.

Previous global estimates of shelf export exist for DIN and DIP (Sharples et al., 2017), DON and DOC (Rabouille et al., 2001), and DSi (Laruelle et al., 2009). Sharples et al. (2017) estimated 75% of riverine DIN, and 80% of riverine DIP is exported to the open ocean, which is higher than our estimate of 2.8–44.3% DIN and 3.5–45.9% DIP. We estimate similar global patterns of export timescales as Sharples et al. (2017), with efficient export near the equator and low export efficiency at the high latitudes. However, even assuming conservative export, our estimates of nutrient export are much lower than the estimates of Sharples et al. (2017). The discrepancy results from different approaches to calculating export. Sharples et al. (2017) assumed that all of the plume water crosses the shelf break when $S_p \geq 1$ ($E_X^{FW} = 1$) and then estimate nutrient removal using empirical relationships that are a function of the export timescale. In contrast, we take into account not only the export timescale but also the plume circulation. As a result, freshwater export efficiency is less than 1 for most rivers, because even for plumes that reach the shelf break ($S_p \geq 1$), not all plume water is exported.

The global mass balance models by Rabouille et al. (2001) for DON and DOC and Laruelle et al. (2009) for DSi also predict much lower riverine export of nutrients than Sharples et al. (2017). Globally, Rabouille et al. (2001) estimate that 7% riverine DON and 15% riverine DOC are exported to the open ocean. We estimate a range of 5.6–51.8% and 5.7–52.2% export for DON and DOC, respectively. Our low estimates correspond to nonconservative export and agree with those of Rabouille et al. (2001). Our estimate of riverine DSi export is 7.0–56.4%. Again, the low estimate corresponding to nonconservative behavior agrees with that of Laruelle et al. (2009), who estimate global export to the deep ocean of 9% (the riverine fraction of export), suggesting global removal of DSi on shelves is high. It should be noted that the models of Rabouille et al. (2001) and Laruelle et al. (2009) only assess globally averaged values. Our framework provides similar estimates, while at the same time providing means of determining spatial patterns of export.

Each of these comparisons, from individual rivers to the global continental shelf, highlights the usefulness of the simple methodology for estimating riverine export to the open ocean, while illustrating the challenges of the simplified approach. Our method addresses solely the riverine component of shelf nutrient budgets; it does not include other shelf processes that are external to river plume dynamics, such as onwelling of deep ocean nutrients. Our estimates of cross-shelf export of riverine materials are in general agreement with the previous literature (e.g., DeMaster & Aller, 2001; Laruelle et al., 2009; Rabouille et al., 2001; Zhang et al., 2012) except for the global nutrient export calculated by Sharples et al. (2017). The methodology is useful in providing a simple estimate of the riverine contribution to open ocean regions as well as in identifying regions especially prone to the negative effects of eutrophication and hypoxia because of high shelf retention.

5. Conclusions

Using relationships described in Izett and Fennel (2018) that relate the efficiency of river plume export to the open ocean to the ratio of a plume's Rossby radius to the local shelf width, we estimated the global export of fresh water and nutrients. Overall, we estimate that just 15–53% of the total riverine fresh water is transported to the open ocean, with much lower export for nutrients due to biogeochemical processing that occurs on the shelves. DSi is exported most efficiently of the nutrients considered with a global estimate of 7.0–56.7%, while DIN is least efficiently exported with just 2.8–44.3% of riverine input reaching the open ocean due to the latitudinal variation of nutrient delivery.

Global variations in nutrient delivery and export patterns are obvious. Cross-shelf export is most efficient within 20° of the equator where riverine material is most directly transported across the shelf (due to the lack of Coriolis force). At higher latitudes, long export timescales and inefficient cross-shelf transport result in very small direct exports of riverine material to the open ocean. Inefficient nutrient export also corresponds to global hypoxic zones, such as the Gulf of Mexico, where nutrients remain on the shelf and are available for enhanced production.

The primary advantage of the methods outlined in this work is their simplicity and generality. The relationships between the ratio of Rossby radius to shelf width and export can be used to estimate riverine export for any river—as demonstrated here—allowing for a straightforward global estimate of nutrient export that can easily be incorporated within global ocean and Earth system models.

Acknowledgments

We are grateful to Jonathan Sharples for his willingness to share and discuss his results throughout the preparation and completion of this research. We also thank Rachel Horwitz, Jinyu Sheng, Chris Algar, and Michael Whitney for comments on an earlier draft of this manuscript. J. I. was funded through the NSERC CGS-M award and the Nova Scotia Scholarship. K. F. acknowledges funding from the NSERC Discovery Program. All data are included in the supporting information as Data Set S1 (including river locations and inputs, shelf widths, and estimated export values).

References

- Amante, C., & Eakins, B. W. (2009). ETOPO1 1 arc-minute global relief model: Procedures, data sources and analysis. NOAA Technical Memorandum NESDIS NGDC-24.
- Bernard, C. Y., Dürr, H. H., Heinze, C., Segsneider, J., & Maier-Reimer, E. (2011). Contribution of riverine nutrients to the silicon biogeochemistry of the global ocean – A model study. *Biogeosciences*, 8, 551–564. <https://doi.org/10.5194/bg-8-551-2011>
- Chen, C.-T., Liu, K.-K., & MacDonald, R. (2003). Continental margin exchanges. In M. J. Fasham (Ed.), *Ocean Biogeochemistry*, (pp. 53–97). Verlag: Springer. https://doi.org/10.1007/978-3-642-55844-3_4
- Cotrim da Cunha, L., Buitenhuis, E. T., Le Quéré, C., Giraud, X., & Ludwig, W. (2007). Potential impact of changes in river nutrient supply on global ocean biogeochemistry. *Global Biogeochemical Cycles*, 21, GB4007. <https://doi.org/10.1029/2006GB002718>
- DeMaster, D. J., & Aller, R. C. (2001). Biogeochemical processes on the Amazon shelf: Changes in dissolved and particulate fluxes during river/ocean mixing. In M. E. McClain, R. L. Victoria, & J. E. Richey (Eds.), *The Biogeochemistry of the Amazon Basin* (pp. 328–357). New York: Oxford Univ. Press.
- Diaz, R. J., & Rosenberg, R. (2008). Spreading dead zones and consequences for marine ecosystems. *Science*, 321, 926–929. <https://doi.org/10.1126/science.1156401>
- Doney, S. C. (2010). The growing human footprint on coastal and open-ocean biogeochemistry. *Science*, 328, 1512–1516. <https://doi.org/10.1126/science.1185198>
- Fennel, K., Wilkin, J., Levin, J., Moisan, J., & O'Reilly, J. (2006). Nitrogen cycling in the Middle Atlantic Bight: Results from a three-dimensional model and implications for the North Atlantic nitrogen budget. *Global Biogeochemical Cycles*, 20, GB3007. <https://doi.org/10.1029/2005GB002456>
- Galloway, J. N., Dentener, F. J., Capone, D. G., Boyer, E., Howarth, R., Seitzinger, S. P., ... Vöös, M. (2004). Nitrogen cycles: Past, present, and future. *Biogeochemistry*, 70, 153–226. <https://doi.org/10.1007/s10533-004-0370-0>
- Garvine, R. W., & Whitney, M. M. (2006). An estuarine box model of freshwater delivery to the Coastal Ocean for use in climate models. *Journal of Marine Research*, 64(2), 173–194. <https://doi.org/10.1357/00222400677606506>
- Gruber, G., & Galloway, J. N. (2008). An earth-system perspective of the global nitrogen cycle. *Nature*, 451(7176), 293–296. <https://doi.org/10.1038/nature06592>
- Izett, J., & Fennel, K. (2018). Estimating the cross-shelf export of riverine materials: Part 1. General relationships from an idealized numerical model. *Global Biogeochemical Cycles*, 32, 160–175. <https://doi.org/10.1002/2017GB005667>
- Jickells, T. D., Buitenhuis, E., Altieri, K., Baker, A. R., Capone, D., Duce, R. A., ... Zamora, L. M. (2017). A reevaluation of the magnitude and impacts of anthropogenic atmospheric nitrogen inputs on the ocean. *Global Biogeochemical Cycles*, 31, 289–305. <https://doi.org/10.1002/2016GB005586>
- Laruelle, G. G., Robeix, V., Sferratore, A., Brodherr, B., Ciuffa, D., Conley, D. J., ... Van Cappellen, P. (2009). Anthropogenic perturbations of the silicon cycle at the global scale: Key role of the land-ocean transition. *Global Biogeochemical Cycles*, 23, GB4031. <https://doi.org/10.1029/2008GB003267>
- Lehrter, J. C., Ko, D. S., Murrell, M. C., Hagy, J. D., Schaeffer, B. A., Greene, R. M., ... Penta, B. (2013). Nutrient distributions, transports, and budgets on the inner margin of a river-dominated continental shelf. *Journal of Geophysical Research: Oceans*, 118(10), 4822–4838. <https://doi.org/10.1002/jgrc.20362>
- Mayorga, E., Seitzinger, S. P., Harrison, J. A., Dumont, E., Beusen, A. H., Fekete, A. F., ... Van Drecht, G. (2010). Global nutrient export from WaterSheds2 (NEWS2): Model development and implementation. *Environmental Modelling and Software*, 25, 837–853. <https://doi.org/10.1016/j.envsoft.2010.01.007>
- Rabouille, C. F., Mackenzie, T., & Ver, L. M. (2001). Influence of the human perturbation on carbon, nitrogen, and oxygen on biogeochemical cycles in the global coastal ocean. *Geochimica et Cosmochimica Acta*, 65(21), 3615–3641. [https://doi.org/10.1016/S0016-7037\(01\)00760-8](https://doi.org/10.1016/S0016-7037(01)00760-8)
- Seitzinger, S. P., Mayorga, E., Bouwman, A. F., Kroeze, C., Beusen, A. H., Billen, G., ... Harrison, J. A. (2010). Global river nutrient export: A scenario analysis of past and future trends. *Global Biogeochemical Cycles*, 24, GB0A08. <https://doi.org/10.1029/2009GB003587>
- Sharples, J., Middelburg, J. J., Fennel, K., & Jickells, T. D. (2017). What proportion of riverine nutrients reaches the open ocean? *Global Biogeochemical Cycles*, 31, 39–58. <https://doi.org/10.1002/2016GB005483>
- Xue, Z., He, R., Fennel, K., Cai, W.-J., Lohrenz, S., & Hopkinson, C. (2013). Modelling ocean circulation and biogeochemical variability in the Gulf of Mexico. *Biogeosciences*, 10(11), 7219–7234. <https://doi.org/10.5194/bg-10-7219-2013>
- Zhang, X., Hetland, R. D., Marta-Almeida, M., & DiMarco, S. F. (2012). A numerical investigation of the Mississippi and Atchafalaya freshwater transport, filling and flushing times on the Texas-Louisiana shelf. *Journal of Geophysical Research*, 117, C11009. <https://doi.org/10.1029/2012JC008108>